Collagen Analysis at Terahertz Band using Double-Debye Parameter Extraction and Particle Swarm Optimisation

Ke Yang, *Member, IEEE,* Nishtha Chopra, *Member, IEEE,* Qammer H. Abbasi, *Senior Member, IEEE,* Khalid Qaraqe, *Senior Member, IEEE,* and Akram Alomainy, *Senior Member, IEEE,*

***Abstract*—The paper focuses on the analysis of cultivated collagen samples at the terahertz (THz) band using double debye model parameter extraction. Based on measured electrical and optical parameters, we propose a model to describe such parameters extracted with a global optimisation method; namely, Particle Swarm Optimisation (PSO). Comparing the measured data with ones in the open literature, it is evident that using only cultivated collagen is not sufficient to represent the performance of the epidermis layer of the skin tissue at the THz band of interest. The results show that the differences between the measured data and published ones are as high as 14 and 6 for the real and imaginary values of the dielectric constant, respectively. Our proposed double debye model agrees well with the measured data.**

***Index Terms*—Nano Communication, Terahertz, Double-Debye model, permittivity.**

I. Introduction

Body-centric wireless communication at the nano-scale, along with internet-of-nanothings, is receiving substantial interests for various disciplines [1]–[3]. Based on recent advancement in carbon nano-tube technologies and Graphene applications, the THz band presents a promising operation frequency of such nano-scale networks specifically for the EM paradigm in communication between nano-devices inside/outside the human body. As an essential first step in studying body-centric nano-networks, it is important to characterise human tissues at the THz frequency band considering that reported results in the open literature are very limited and application/environment-specific. Pulsed THz spectroscopy was first used to measure the absorptance of DNA, bovine serum albumin and collagen at the band of 0.06 to 2.0 THz [4], showing that the absorption would increase with hydration and denaturing. Later, animal tissues, such as pork skin, pork fat and rat skin, were measured to study the power absorption and far-infrared signal transmission at the THz band [5].

Due to variation in molecular structures within the cancerous tissue compared to a healthy one, their electrical and optical parameters are different within the THz band. Therefore, substantial numbers of studies are conducted to characterise such variations in terms of reflection and transmission of such tissue types in the open literature. Healthy and cancerous liver tissues were studied to indicate the possibility of the application of THz Fiber-scanning Near-Field Imaging technology to diagnose cancer [6]. Recently, spectroscopy measurements of normal and cancerous breast tissue in the range of 0.1 to 4 THz were conducted by Tyler Bowman and *et. al.* [7], demonstrating the potential of THz spectroscopy for the recognition of the cancerous cell while the dielectric model of human breast tissue in the THz band was built by A.J. Fitzgerald [8]. The average complex permittivity of healthy tumour, healthy fibrous breast tissue and healthy fat breast tissue from [9] were compared. Later, the same comparison between normal skin tissues and cancerous ones was conducted in [10]. Considering there are a few studies in the open literature with regards to human tissue characterisation of electrical and optical parameters [11]–[14], further investigations are required with varying level of complexity in tissue structures since the devices are envisioned at the nano-scale [15], [16]. It is also important to consider tissue state from hydration and tension prospective. In the proposed study, we investigate the applicability of cultivated collagen to be used as a replacement of real skin tissue samples. The cultivated collagen obtained from the Blizard Institute is characterised using the THz Time Domain Spectroscopy (THz-TDS) system housed in Queen Mary University of London [17]. Thereafter, the extracted electrical parameters of cultivated collagen are compared with those of the real skin to investigate similarity and reliability of using such artificial samples as a replacement to the real ones. Based on the measured parameters, the double-debye model is further proposed to describe the data along the whole band and the particle swarm optimisation method is applied to extract the corresponding parameters.

The rest of the paper is organised as follows. In Section II, the fundamentals of the experiment like sample preparation and system set-up are introduced. While in Section III, the measured data are processed to obtain the dielectric constant of the cultivated collagen, followed by the modelling of the results in Section IV. In the end, a brief conclusion is drawn.

II. Fundamentals of the Experiment

A. Sample Preparation

Rat-tail type I collagen, which is the most abundant of the collagen and exists in tendons, skin, ligaments and many

Ke Yang, Nishtha Chopra and A. Alomainy are with School of Electronic Engineering and Computer Science, Queen Mary University of London, London; e-mail: {k.yang;n.chopra;a.alomainy}@qmul.ac.uk.

Qammer and Khalid are with the Dep. of Electrical and Computer Engineering, Texas A & M University at Qatar. Qammer is also with Queen Mary University of London and UET, Lahore; e-mail: {qammer.abbasi;k.qaraqe}@tamu.edu.

interstitial connective tissues, is applied as a base reagent for gel preparation. The fibroblast cells are added to Fetal Bovine Serum (FBS), which could supply essential nutrients for the cell growth. In addition, the concentrated Modified Eagles Medium (MEM), which also contains a balance of nutrients to feed the fibroblasts is added to the mixture of the collagen and fibroblast. A small quantity of sodium hydroxide is later added wisely to the mixed solution to set the gel until the pH indicator in the MEM turns pink. The gel is then incubated (5% CO_2) for gelation at 37^oC for approximately 45 min. Once the initial gelation takes place, the diameter of the mixture is measured to observe any signs of contraction. Kept in an incubator for almost a week, the diameter of the gel should be measured constantly to make it contract to its maximum value. Subsequently, the gel, shown in Fig. 1 is kept in the refrigerator to keep fresh.

Fig. 1. Collagen sample prepared in Blizard Institute [17]

B. Terahertz Time Domain Spectroscopy System Set-up

A schematic illustration of the set-up of a Terahertz Time Domain Spectroscopy System (THz-TDS) in transmission mode used in this work is shown in Fig. 2. The pulsed titanium-sapphire laser produces femtosecond pulses, which are then redirected into two separate optical paths by a beam-splitter. One beam becomes the receiver pulse (a measurement using the receiver is possible only when a femtosecond pulse is incident on the receiver), while the other is used to excite THz wave at the emitter. Parabolic mirrors are used to focus and collimate the THz pulses travelling through the sample and onto the detector. The detector only conducts when it is struck by the femtosecond pulse from the detection beam line. When the detector is photo-excited, the THz pulses electric field causes an electric current to flow inside the detector. The time delay on the detector beam line is used to control the relative time delay between the THz pulses. When the detector can conduct, the electric field of the THz pulses can be plotted over time.

The photo of the THz-TDS installed at QMUL is shown in Fig. 3. The system shown here is operating in transmission mode. The main features and characteristics of this spectrometer are [19]:

- Typical operating frequency domain: $0.1 - 4.0\ THz$;

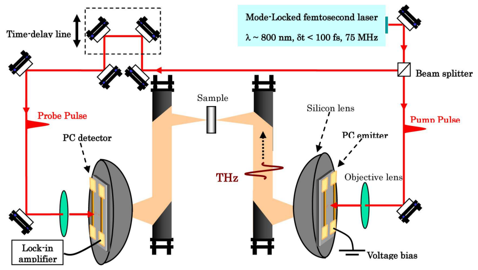

Fig. 2. Schematic diagram of a THz-TDS system operating in transmission mode [18]

- Maximum dynamic range is $25-30\ dB$, SNR is normally around $25\ dB$;
- Motorized delay stage maximum travelling distance is $15\ cm$;
- Typical resolution is $14\ GHz$ (scan size $10.24\ mm$, step $10\ \mu m$); maximum achievable resolution is $1-2\ GHz$;

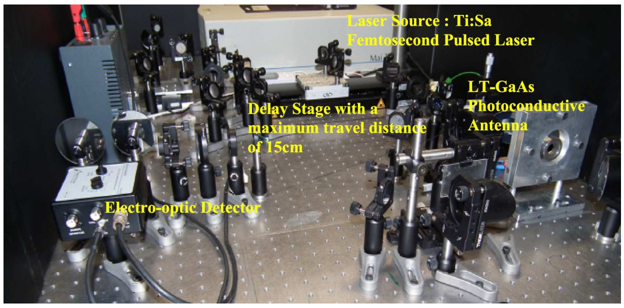

Fig. 3. THz-TDS system in Queen Mary University of London [17], [19]

After the collagen sample is cultivated in Blizard Institute, it is kept in an iced box and taken to the THz lab in QMUL. The samples would be measured with the THz-TDS system within a day. During the experiment, the system without the holder is measured first to get the time-domain pulse response of the air and then the response of system with empty holder, made of poly-4-methyl pentene-1 (TPX) with low absorption ($\leq 1cm^{-1}$) and almost constant refractive index (1.46) over the band of interest. Finally, the holder with the sample is measured. For each step, the measurement is repeated 3 times to get the mean value; also, for each sample with different thickness, three measurements are conducted and the mean value of the final results is adopted. Dry air or nitrogen is pumped into the system to eliminate the effects of the vapour.

III. Date Processing and Measured Results

A. Data-Processing

The original measurement data from the THz-TDS system are the received electric field $\vec{E}$. The complex spectra of air measured by TDS system is shown in Fig. 4.

Conventionally, the rate of the sample spectra to the reference one, which is served by the absence of the sample, usually the air, is used to calculate the complex refractive index $\tilde{n} = n - i\kappa$. Thus, the measured transfer function is:

$$\tilde{H}_{measure}(f) = \frac{\tilde{E}_{sam}(f)}{\tilde{E}_{ref}(f)} \tag{1}$$

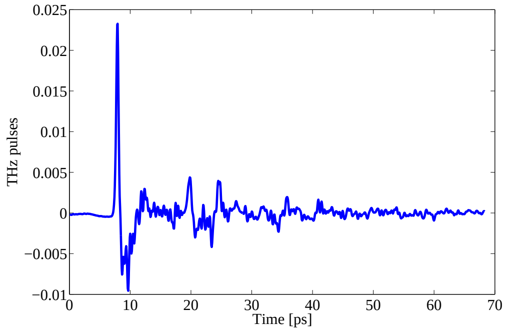

Fig. 4. Received THz pulse of air from TDS system

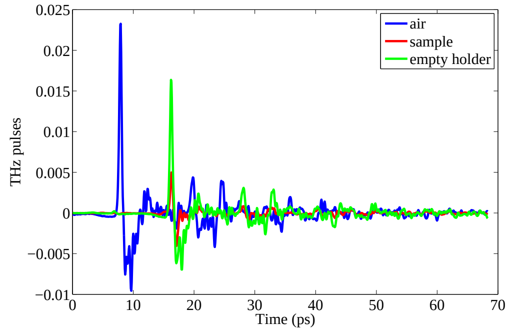

Fig. 5. Time response of air, empty holder and the holder with the sample measured by THz-TDS system

where, $\tilde{E}_{sam}(f)$ and $\tilde{E}_{ref}(f)$ are the complex spectra of the sample and reference, obtained from the Fourier Transform of the corresponding time-domain response.

Since the THz wave arriving at the sample is regarded as the TE wave, thus the propagation of the wave through the sample can be described by [19]:

$$\tilde{A} = e^{-\frac{i2\pi f \tilde{n} d}{c}} \tag{2}$$

where, f is the frequency; $\tilde{n}$ is the complex refractive index; d is the sample thickness; c is the speed of light in free space.

Therefore, the analytical transfer function can be obtained [19]:

$$\tilde{H}(f) = \tilde{t}_{12}(f)\tilde{t}_{21}(f)e^{-\frac{i2\pi f(\tilde{n}-n_{air})d}{c}} \tag{3}$$

where, f is the frequency; $\tilde{n}$ is the complex refractive index; n_{air} is the refractive index of air because air is usually taken as the reference; d is the sample thickness; c is the free-space light speed; $\tilde{t}_{12}(f)$ and $\tilde{t}_{21}(f)$ are the Fresnel transmission coefficients associated with the front and back boundary interfaces between sample and holder medium. Then, the non-linear regression algorithm is applied to obtain the complex refractive index.

B. Measured Results and Discussions

Fig. 5 shows the measured time response of air, empty holder and the holder with the sample, from which we can see that the inclusion of holder causes considerable delay and slight attenuation of the pulse compared to the air while the sample introduced slight delay and considerable attenuation compared to the empty holder. By doing the *Fourier Transform* and non-linear regression algorithm, the refractive index and extinction coefficient can be obtained, as shown in Fig. 6. We can see that with the rise of the frequency, the refractive index and extinction coefficient both decrease. Before $0.5\ THz$, both parameters descend steeply while after $0.5\ THz$ both parameters drop slightly.

Using the following relationship between the EM parameters to the optical parameters, Eq. 4, the permittivity of the collagen can be obtained, as shown in Fig. 7. Similar to the optical parameters, the permittivity decreases with the increase of the frequency and there is also a frequency point, $0.5\ THz$ approximately, where the trend of both curves change.

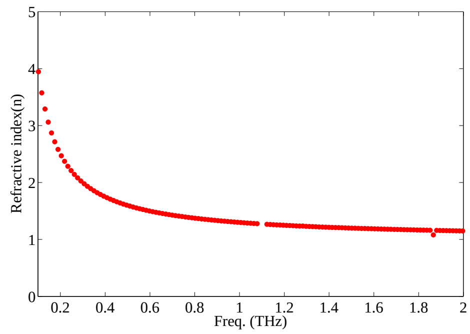

(a) Relative refractive index measured by THz-TDS system

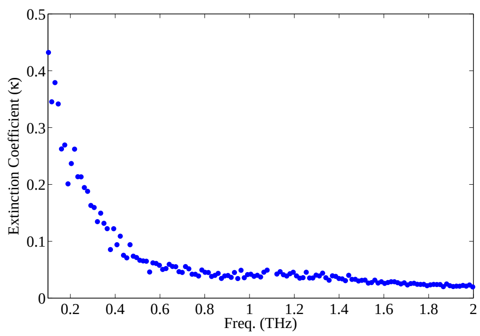

(b) Extinction coefficient measured by THz-TDS system

Fig. 6. Measured optical parameters of collagen from THz-TDS system

$$\begin{cases} \epsilon' = n_r(f)^2 - \kappa(f)^2 \\ \epsilon'' = 2n_r(f)\kappa(f) \end{cases} \tag{4}$$

where, ϵ' and ϵ'' are the real and imaginary part of the permittivity ϵ.

The comparison between the measured results with the data shown in [20], [21] and [22] is shown in Fig. 8. From the figure, it can be easily seen that although the trend of the three curves is similar, the permittivity of the measured collagen is less than the others' data, demonstrating that the collagen is not enough to represent the epidermis at the band of interest. The difference between the measured data and the available literature at the lower band is quite enormous, where the

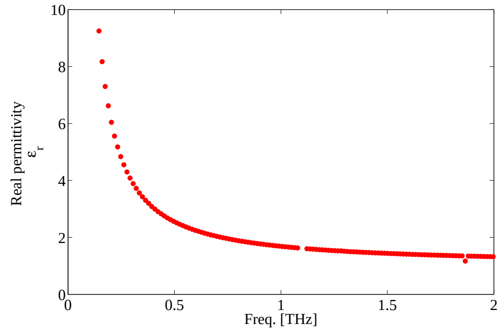

(a) Real part of the dielectric constant measured by THz-TDS system

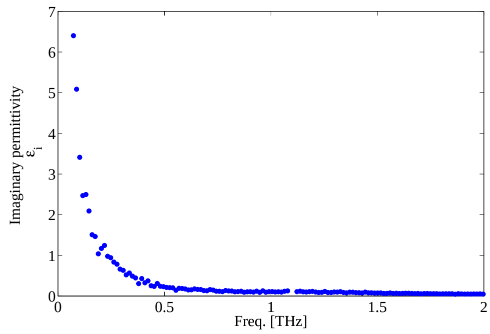

(b) Imaginary part of the dielectric constant measured by THz-TDS system

Fig. 7. Calculated complex dielectric constant of collagen from Eq. 4

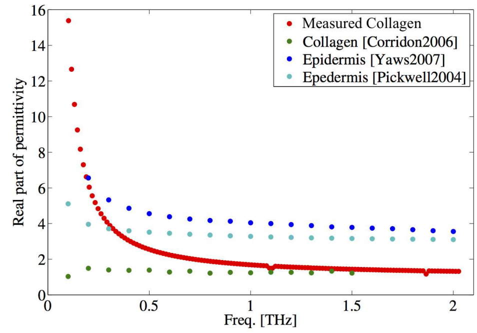

(a) Comparison of the real part of the dielectric constants of skin

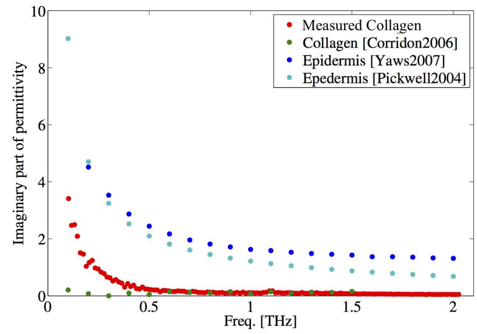

(b) Comparison of the imaginary part of the dielectric constants of skin

Fig. 8. Comparison between the measured results with other avaiblable data from [20]–[22]

highest one could go up to 14 and 6 for the real part and imaginary part of the dielectric constant. Also, it is worth noticing that the trend of data in [21] is different from others in the lower frequency band, which is mainly due to the fact that the used samples are dehydrated.

IV. Modelling of the Measured Results

A. Dielectric Model of Collagen at THz Band

As stated before, the human tissue is always considered as a dispersive material; thus, relative permittivity and conductivity should be both included in the model. And from the previous section, it can be easily seen that the frequency rise will cause a drop of the permittivity. Therefore, Debye model, as shown in Eq. 5 would be appropriate to express the dependence of dielectric properties on the frequency. Complex permittivity of human tissue in the very low frequency range is well-described by the single-debye relaxation model, while its responses in higher frequencies above 0.1 THz require extra Debye relaxation process [23] because of the higher water content of various human tissues [14].

$$\epsilon_\omega = \epsilon_\infty + \sum_n \frac{\Delta\epsilon_n}{1 + j\omega\tau_n} \tag{5}$$

where $\Delta\epsilon_n$ is the difference between static permittivity and permittivity at higher frequencies $\epsilon_s - \epsilon_\infty$, indicating the permittivity dispersion of the nth-Debye relaxation process; ω is the angular frequency and ϵ_∞, τ_n are the permittivity at infinite frequency and relaxation time.

The double-Debye model, shown in Eq. 6 was first applied to describe the dielectric function of water, and then has been widely used for highly hydrated mixtures [24], [25]. In [26], it has already been used as the function to describe the interaction of THz radiation with human skin tissue.

$$\epsilon_\omega = \epsilon_\infty - \frac{\Delta\epsilon_1}{1 + j\omega\tau_1} + \frac{\Delta\epsilon_2}{1 + j\omega\tau_2} \tag{6}$$

where ϵ_∞ is the permittivity at infinite frequency, larger than the vacuum permittivity ϵ_0. $\Delta\epsilon_1$ represents the dispersion in amplitude of the slow relaxation processes, where the bulk bonding between hydrogen molecules is released to equilibrium state under the impact of external electric field. $\Delta\epsilon_2$ describes the fast relaxation process, where hydrogen-bond formation and decomposition occur. τ_1 is the relaxation time of the slow process and τ_2 is the relaxation time of the fast process [25]. ω is the angular frequency.

B. Fitting Algorithm

To obtain the parameters of *Double-Debye Model*, the Euclidean distance [27] between the raw data input and the Eq. 6 output was employed, shown in Eq. 7:

$$e = \frac{1}{N}\sum_{i=1}^{N}[(\frac{\epsilon'_{\omega_i} - \hat{\epsilon}'_{\omega_i}}{median[\epsilon'_{\omega_i}]})^2 + (\frac{\epsilon''_{\omega_i} - \hat{\epsilon}''_{\omega_i}}{median[\epsilon''_{\omega_i}]})^2] \tag{7}$$

where ϵ'_{ω_i} and ϵ''_{ω_i} are the real and imaginary part of measured dielectric properties. $\hat{\epsilon}'_{\omega_i}$ and $\hat{\epsilon}''_{\omega_i}$ represent the output of the

Debye equation for real and imaginary part of the dielectric properties, respectively, and N is the number of points picked across the frequency range of 0.1 THz to 1.5 THz (almost 212 for this study).

The optimisation problem can be summarised as below:

$$\min_{\epsilon_\infty,\Delta\epsilon_1,\Delta\epsilon_2,\tau_1,\tau_2} \frac{1}{N}\sum_{i=1}^{N}[(\frac{\epsilon'_{\omega_i}-\hat{\epsilon}'_{\omega_i}}{median[\epsilon'_{\omega_i}]})^2+(\frac{\epsilon''_{\omega_i}-\hat{\epsilon}''_{\omega_i}}{median[\epsilon''_{\omega_i}]})^2]$$
$$\text{subject to} \quad \epsilon_\infty \geq 1, \quad \Delta\epsilon_1 \geq 0, \Delta\epsilon_2 \geq 0, \quad \tau_1 \geq 0, \tau_2 \geq 0 \tag{8}$$

To solve this problem, particle swarm optimisation (PSO) [28] was applied, which would return all Double Debye variables for the five set of parameters if the Euclidean distance is smaller than the defined threshold of 0.0012.

The number of particles chosen in the PSO algorithm here is 500. The algorithm would end after 1000 iterations if the threshold is not reached before this point. The final parameters of the Double Debye Model are shown in Table I and Fig. 9 demonstrates the comparison between the complex permittivity calculated from the double debye model and the measured data for collagen, showing that the proposed dielectric model mimics very well the dielectric properties of collagen not only at the high range of frequency (beyond 1 THz) but also at the lower band.

TABLE I
PARAMETERS OF DOUBLE DEBYE MODEL OPTIMISED BY PSO ALGORITHM

ϵ_∞	$\Delta\epsilon_1$	τ_1 (ps)	$\Delta\epsilon_2$	τ_2 (ps)
1.63	500	17.7	100	3.64

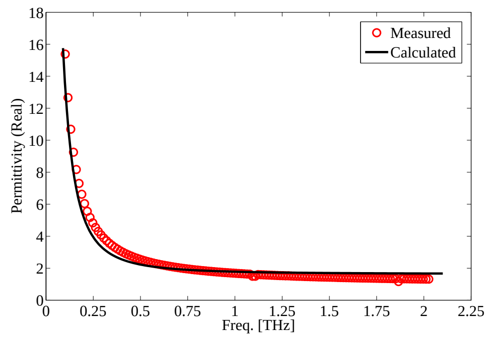

(a) Real part of the permittivity

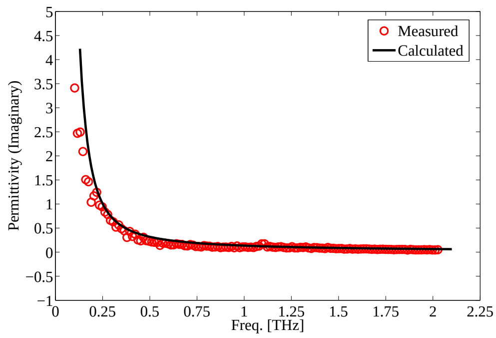

(b) Imaginary part of the permittivity

Fig. 9. Measured complex permittivity of collagen and its fitting model

V. CONCLUSION

The possibility of using the collagen as a true replacement to the real skin numerically and experimentally is investigated in the paper, by comparing the measured results to the available data, showing that the cultivated collagen in its simple format is not sufficient to represent the real skin at the band of interest. In addition, a double-debye model is proposed and the corresponding parameters are extracted by the particle swarm optimisation technique. The proposed model shows good agreement with the measured data and hence demonstrating confidence in the application of such models in representing the electrical and optical parameters of artificial collagen at the band of interest.

ACKNOWLEDGEMENT

This publication is made possible by NPRP grant # 7-125-2-061 from the Qatar National Research Fund (a member of Qatar Foundation). The statements made herein are solely the responsibility of the authors.

REFERENCES

[1] Ke Yang, Alice Pellegrini, Max O Munoz, Alessio Brizzi, Akram Alomainy, and Yang Hao. Numerical analysis and characterization of thz propagation channel for body-centric nano-communications. *Tera-Hertz Science and Technology, IEEE Transaction on*, 2015.

[2] Qammer H. Abbassi, Masood Ur Rehman, Khalid Qaraqe, and Akram Alomainy. *Advances in Body-Centric Wireless Communications: Applications and Stateof- the-art*. The Institution of Engineering and Technolog (IET) Publication, July 2016.

[3] Q. H. Abbasi, K. Yang, N. Chopra, J. M. Jornet, N. A. Abuali, K. A. Qaraqe, and A. Alomainy. Nano-communication for biomedical applications: A review on the state-of-the-art from physical layers to novel networking concepts. *IEEE Access*, 4:3920–3935, 2016.

[4] AG Markelz, A Roitberg, and EJ Heilweil. Pulsed terahertz spectroscopy of dna, bovine serum albumin and collagen between 0.1 and 2.0 thz. *Chemical Physics Letters*, 320(1):42–48, 2000.

[5] Mingxia He, Abul K Azad, Shenghua Ye, and Weili Zhang. Far-infrared signature of animal tissues characterized by terahertz time-domain spectroscopy. *Optics Communications*, 259(1):389–392, 2006.

[6] Chen Hua, Ma Shi-Hua, Yan Wen-Xing, Wu Xiu-Mei, and Wang Xiao-Zhou. The diagnosis of human liver cancer by using thz fiber-scanning near-field imaging. *Chinese Physics Letters*, 30(3):030702, 2013.

[7] Tyler Bowman, Magda El-Shenawee, and Shubhra Gautam Sharma. Terahertz spectroscopy for the characterization of excised human breast tissue. In *Microwave Symposium (IMS), 2014 IEEE MTT-S International*, pages 1–4. IEEE, 2014.

[8] Bao CQ Truong, Hoang D Tuan, Anthony J Fitzgerald, Vincent P Wallace, and Hung T Nguyen. A dielectric model of human breast tissue in terahertz regime. *Biomedical Engineering, IEEE Transactions on*, 62(2):699–707, 2015.

[9] Philip C Ashworth, Emma Pickwell-MacPherson, Elena Provenzano, Sarah E Pinder, Anand D Purushotham, Michael Pepper, Vincent P Wallace, et al. Terahertz pulsed spectroscopy of freshly excised human breast cancer. *Optics express*, 17(15):12444–12454, 2009.

[10] Bao CQ Truong, Hoang Duong Tuan, Vincent P Wallace, Anthony J Fitzgerald, and Hung T Nguyen. The potential of the double debye parameters to discriminate between basal cell carcinoma and normal

skin. *IEEE Transactions on Terahertz Science and Technology*, 5(6):990–998, 2015.

[11] Ronald Pethig. Dielectric properties of biological materials: Biophysical and medical applications. *Electrical Insulation, IEEE Transactions on*, (5):453–474, 1984.

[12] Camelia Gabriel, Sami Gabriel, and E Corthout. The dielectric properties of biological tissues: I. literature survey. *Physics in medicine and biology*, 41(11):2231, 1996.

[13] S Gabriel, RW Lau, and Camelia Gabriel. The dielectric properties of biological tissues: Ii. measurements in the frequency range 10 hz to 20 ghz. *Physics in medicine and biology*, 41(11):2251, 1996.

[14] Sami Gabriel, RW Lau, and Camelia Gabriel. The dielectric properties of biological tissues: Iii. parametric models for the dielectric spectrum of tissues. *Physics in medicine and biology*, 41(11):2271, 1996.

[15] Q. H. Abbasi, H. El Sallabi, N. Chopra, K. Yang, K. A. Qaraqe, and A. Alomainy. Terahertz channel characterization inside the human skin for nano-scale body-centric networks. *IEEE Transactions on Terahertz Science and Technology*, 6(3):427–434, May 2016.

[16] Ke Yang, Qammer Hussain Abbasi, Nishtha Chopra, Max Munoz, Yang Hao, and Akram Alomainy. Effects of non-flat interfaces in human skin tissues on the in-vivo tera-hertz communication channel. *Nano Communication Networks*, 8:16 – 24, 2016. Electromagnetic Communication in Nano-scale.

[17] Nishtha Chopra, Ke Yang, Jamie Upton, Qammer Hussain Abbasi, Khalid Qaraqe, Mike Philpott, and Akram Alomainy. Fibroblasts cell number density based human skin characterization at {THz} for in-body nanonetworks. *Nano Communication Networks*, 10:60 – 67, 2016. Terahertz Communications.

[18] Terahertz Time Domain Spectroscopy System. http://fir.u-fukui.ac.jp/thzlab/index_files/Eng_THz_TDS.htm.

[19] Oleksandr Sushko. *Terahertz dielectric study of bio-molecules using time-domain spectrometry and molecular dynamics simulations*. PhD thesis, School of Electronic Engineering and Computer Science, Queen Mary University of London, March 2014.

[20] KM Yaws, DG Mixon, and WP Roach. Electromagnetic properties of tissue in the optical region. In *Biomedical Optics (BiOS) 2007*, pages 643507–643507. International Society for Optics and Photonics, 2007.

[21] Peter M Corridon, Ricardo Ascázubi, Courtney Krest, and Ingrid Wilke. Time-domain terahertz spectroscopy of artificial skin. In *Biomedical Optics 2006*, pages 608007–608007. International Society for Optics and Photonics, 2006.

[22] E Pickwell, BE Cole, AJ Fitzgerald, M Pepper, and VP Wallace. In vivo study of human skin using pulsed terahertz radiation. *Physics in Medicine and Biology*, 49(9):1595, 2004.

[23] Hans J Liebe, George A Hufford, and Takeshi Manabe. A model for the complex permittivity of water at frequencies below 1 thz. *International Journal of Infrared and Millimeter Waves*, 12(7):659–675, 1991.

[24] SW Smye, JM Chamberlain, AJ Fitzgerald, and E Berry. The interaction between terahertz radiation and biological tissue. *Physics in medicine and biology*, 46(9):R101, 2001.

[25] E Pickwell, BE Cole, AJ Fitzgerald, VP Wallace, and M Pepper. Simulation of terahertz pulse propagation in biological systems. *Applied Physics Letters*, 84(12):2190–2192, 2004.

[26] Bao CQ Truong, Hoang Duong Tuan, Ha Hoang Kha, and Hung T Nguyen. Debye parameter extraction for characterizing interaction of terahertz radiation with human skin tissue. *Biomedical Engineering, IEEE Transactions on*, 60(6):1528–1537, 2013.

[27] Mariya Lazebnik, Dijana Popovic, Leah McCartney, Cynthia B Watkins, Mary J Lindstrom, Josephine Harter, Sarah Sewall, Travis Ogilvie, Anthony Magliocco, Tara M Breslin, et al. A large-scale study of the ultrawideband microwave dielectric properties of normal, benign and malignant breast tissues obtained from cancer surgeries. *Physics in Medicine and Biology*, 52(20):6093, 2007.

[28] T. Yilmaz, R. Foster, and Yang Hao. Towards accurate dielectric property retrieval of biological tissues for blood glucose monitoring. *Microwave Theory and Techniques, IEEE Transactions on*, 62(12):3193–3204, Dec 2014.